The 15th International Topical Meeting on Nuclear Reactor Thermalhydraulics, NURETH-15 NURETH15-358
Pisa, Italy, May 12-15, 2013

WALL BOILING MODELING EXTENSION TOWARDS CRITICAL HEAT FLUX

C. Lifante[1], Th. Frank[1] and A. Burns[2,3]
[1] ANSYS Germany GmbH, Staudenfeldweg 12, 83624 Otterfing, Germany
[2] ANSYS UK, 97 Milton Park, Abingdon, OX14 4RY, UK
[3] CFD Centre, Leeds University, Clarendon Road, Leeds, LS2 9JT, UK

Conxita.Lifante@ansys.com

ABSTRACT

Some of the current CFD codes simulate wall boiling by means of the so-called RPI or wall heat flux partitioning model, which was originally formulated by Kurul and Podowski [1] from Rensselaer Polytechnical Institute. It was designed to be applied in nucleate sub-cooled boiling applications and moderate gas volume fraction near the heated walls. In this regime it is assumed that convection heat transfer between the wall and the liquid, quenching and evaporation phenomena are taking place. However, convection to the gaseous phase also takes place and this is the main heat transfer mechanism when the wall is mostly covered by the vapour phase.
As a requirement to be able to accurately predict dry-out and Critical Heat Flux (CHF), the wall boiling modelling must include this phenomenon. This is of main importance because, when this occurs, the efficiency of the heat transfer process is suddenly strongly deteriorated leading to a dramatic increase in the surface or cladding material temperature. This is an effect that one may want to avoid in any case in many industrial devices, as for instance in a nuclear reactor. In this case the rise of the surface temperature can cause the failure of the cladding material.
The proposed extension has been implemented in a customized version of ANSYS CFX 14.0 [2] based on an exponential blending function. The solver is able to use the standard RPI model in those zones where gas volume fraction is under a critical value. When this value is reached the new component accounting for convection to the gaseous phase is activated.
In order to evaluate the capabilities and accuracy of the proposed method, two cases from the literature have been chosen and investigated. The first one belongs to the series of the well-known experiments by Bartolomej et al. [3], where cross-sectional averaged gas volume fraction of up to 60% is present, implying a significantly large amount of gas at the wall. Since these measurements do not include values of the other main variables like wall temperature, a second complementary case was analyzed. It was experimentally investigated by Hoyer et al [4]. In this case dry-out conditions occur and lead to a dramatic jump in the wall temperature.
In both cases Best Practice Guidelines [5] were followed as much as possible, e.g. performing grid refinement studies and evaluation of numerical errors. The numerical results were able to reproduce the trends and values of the experiments.

1. INTRODUCTION

The use of the RPI wall boiling model is much extended inside the CFD community. Its wall heat partitioning based on a mechanistic approach allows investigating a variety of cases of interest in the area of nuclear reactor safety. However, its main drawback is that it was derived to be applied in situations with moderate gas content, in the nucleate wall boiling regime. It only considers three mechanisms to extract heat from a heated wall: i.e. convection to the fluid phase, quenching and evaporation. This may be appropriate for many applications. However, if the amount of vapour evaporated near the wall is so high that vapour covers most of the wall surface, this vapour may isolate the wall from the sub-cooled fluid. In such situations, none of those three mechanisms are anymore taking place, or at least are not the main driving processes.

Therefore an extension of the RPI-Wall Boiling was implemented in a customized version of ANSYS CFX 14.0. This extension considers that, when the vapour volume fraction is large enough, a fourth mechanism must be included in the wall heat partitioning, namely convection from the wall to vapour. If the heated wall is fully covered by vapour the heat transfer from the wall is responsible for the increase of vapour temperature due to convection. In addition, since the heat capacity of the vapour is significantly smaller than the one of the liquid, less heat can be transferred in comparison. This leads to a sudden dramatic increase of the wall temperature. This situation is usually undesired, especially in nuclear reactors, where this jump in temperature can cause a failure of the cladding.

2. THE RPI WALL BOILING MODEL

The RPI wall boiling model is based on the so called “Wall Heat Partitioning” algorithm. This means that the total heat transfer between the heated wall and the fluid domain is due to convection to the liquid phase, evaporation and transient conduction to the liquid phase when the bubbles depart from the wall and fresh liquid is in contact with the heated wall (quenching). This partitioning can be mathematically described as follows:

$$Q_w = Q_{convl} + Q_{quench} + Q_{evap} \tag{1}$$

where Q_w represents the total heat flux at the heated wall, Q_{convl} the heat flux transferred due to convection into the liquid phase, Q_{quench} the heat flux due to quenching and Q_{evap} the heat flux due to evaporation of the liquid phase. These values are weighted depending on the amount of vapour present at the wall. In order to do this, two area fractions are defined. They correspond to the area fraction of the wall covered by liquid (A_1) and the area fraction of the wall covered by vapour (A_2). They must sum to unity:

$$1 = A_1 + A_2 \tag{2}$$

They are computed as

$$A_2 = \min\left(\frac{\pi F_2^2 d_w^2}{4} \cdot n, 1\right), A_1 = 1 - A_2 \tag{3}$$

where d_w is the bubble departure diameter, n the nucleation site density and F the influence area factor.

Once the weights are defined one may compute the three components of Eq (1), as

$$Q_{convl} = A_1 h_{convl}(T_w - T_l) \tag{4}$$

$$Q_{quench} = A_2 h_{quench}(T_w - T_l) \tag{5}$$

$$Q_{evap} = \dot{m}_{evap} h_{lv} \tag{6}$$

Further details of the modelling of each of these parameters can be found in [1] [2].

3. EXTENSION OF THE RPI MODEL

As already discussed in the introduction, the formulation presented in Section 2 (from now on called standard RPI model version) is not adequate to solve applications with large vapour content in direct contact to the heated wall. In order to simulate these problems, an extension of the standard RPI model has been implemented. It consists of a modification of Eq. (1), where a fourth wall heat flux component has been added

$$Q_w = Q_{convl} + Q_{quench} + Q_{evap} + Q_{convg} \tag{7}$$

Q_{convg} represents the heat flux transferred to the vapour phase due to convection. The new component is defined by analogy as the one regarding convection to the liquid phase, and is computed as

$$Q_{convg} = A_{convg} h_{convg}(T_w - T_g) \tag{8}$$

The heat transfer coefficient is defined as

$$h_{convg} = \frac{\rho_g c_{p_g} u_g^*}{T_g^+} (T_w - T_g) \tag{9}$$

which is the analogous version of

$$h_{convl} = \frac{\rho_l c_{p_l} u_l^*}{T_l^+} (T_w - T_l) \tag{10}$$

Eq. (10) is used to evaluate the heat transfer coefficient of Eq. (4). In both cases turbulent wall functions are used to compute the alternative velocity scale to the phasic friction velocity (u^*) and the dimensionless phase temperature (T^+). Details of the turbulence model and wall function implementation in ANSYS CFX can be found in [1].

In Eq. (8) one new weight is defined (A_{convg}). In this case the value of A_{convg} does not strictly correspond to a physical partition of the heated wall surface. The component regarding the convection to the gaseous phase is only active when a critical gas volume fraction is reached ($r_{g,crit}$). When the gas volume fraction near the wall is lower than the critical value, the standard RPI model with 3 wall heat flux components is used. When the gas volume fraction is equal to 1, which means that the wall is completely covered by vapour, only the new fourth component is active. Finally when the gas volume fraction is within a range close to the critical one, a blending of the standard and the new formulation is used. To consider these three regimes (standard RPI model, pure convection to gas and blending), the weights in Eq. (4), (5) and (8) have been modified by means of an exponential function:

$$f(r_l) = \begin{cases} 1 - \frac{1}{2} e^{\left[-20\left(r_l - r_{l,crit}\right)\right]} & r_l \geq r_{l,crit} \\ \frac{1}{2}\left(\frac{r_l}{r_{l,crit}}\right)^{20 r_{l,crit}} & r_L < r_{l,crit} \end{cases} \quad (11)$$

where $r_{l,crit} = 1 - r_{g,crit}$. The blending function (11) is illustrated in Figure 1 below.

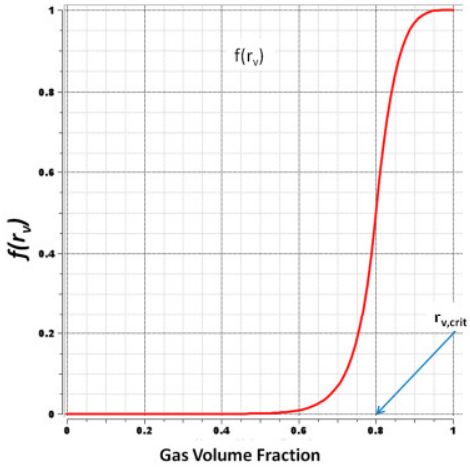

Figure 1 - Exponential function used for blending the standard RPI model and the new non-equilibrium RPI model formulation.

The new weights for each component are then defined as

$$\begin{aligned} A_{convl} &= A_1 * f(r_l) \\ A_{cquench} &= A_2 * f(r_l) \\ A_{evap} &= A_2 * f(r_l) \\ A_{convg} &= 1 - f(r_l) \end{aligned} \quad (12)$$

4. VALIDATION

In order to validate the new implementation two well-known test cases from the literature were chosen: the Bartolomej case [3] and the Hoyer case [4]. They both consist of a vertical pipe with heated outer wall, through which sub-cooled water is flowing upwards. For both cases experimental values are available, and indicate that the amount of vapour near the wall is significantly large. In the Hoyer case even dry-out is occurring. In boiling applications the two most important parameters are the wall temperature and the gas volume fraction. Bartolomej measured gas volume fractions while Hoyer measured wall temperatures. That is the reason to investigate both cases.

4.1 The Bartolomej Case

4.1.1 Case description

Figure 2 shows a sketch of the geometry of the experimental test facility, where Bartolomej conducted his investigations. The working conditions of the selected case are also included in Figure 2.

Bartolomej performed many series of experiments with different boundary conditions [3]. From all of them, we chose the case with the largest amount of gas in the domain. In the original paper by Bartolomej, it can be seen that the cross-sectional averaged values of gas volume fraction reach values of 60 %. This indicates that locally, at the heated wall, these values must be even larger, making the case adequate to test the capabilities of the new implementation.

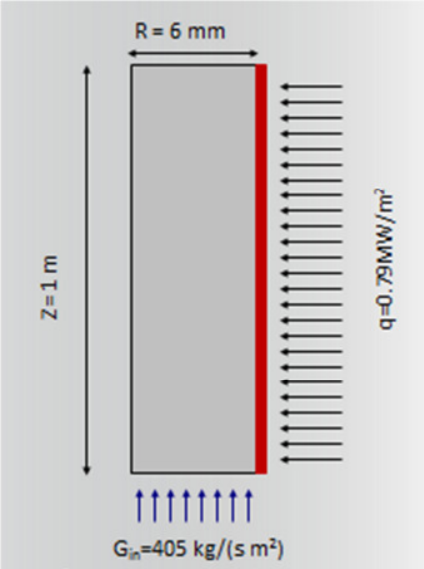

Figure 2 - Sketch of the experimental facility designed by Bartolomej [3].

P	G_{in}	q	Subcooling
7MPa	405 kg/(s m^2)	0.79MW/m^2	90 K

Table 1 - Working conditions of the Bartolomej case.

4.1.2 CFD-Setup

A 2D geometry was considered. The numerical domain was a pipe sector of 1 degree in circumferential direction. Following the Best Practice Guidelines [5] four different grids were generated with a refinement factor of 2 in each coordinate direction. Details of the grid parameters are summarized in Table 2. The finest grid contains 192.000 cells and has a maximum y^+ value of 17 (which is small for a wall boiling simulation).

	Mesh01	Mesh02	Mesh03	Mesh04
Cells	20x150	40x300	80x600	160x1200
Δy^{nw}	0.3 mm	0.15 mm	0.075mm	0.0375mm
Max y^+	115	55	29	17

Table 2 - Parameters of the CFD grids (Bartolomej case)

Standard CFD parameters for multiphase flows [6] were applied. As interfacial forces only drag and lift forces were considered, which were modeled by means of the Grace and Tomiyama laws [1]. It is quite common to assume saturation conditions for the vapour in sub-cooled boiling simulations. However,

since we are investigating a case where convection to vapour is assumed to take place, two phasic energy equations must be solved: one for the liquid and for the vapour phase. Turbulence is modeled by using the SST $k-\omega$ model for the mixture. The interphase heat transfer is modeled applying the Ranz-Marshall model for the liquid [1] and a given Nusselt value for the gas (Nu=26) [7]. The critical gas volume fraction for the activation of the RPI extension was set to be 80% of vapour content.

4.1.3 Results and discussion

Plots in Figure 3 show the results obtained with the finest grid. At the left side the liquid temperature is plotted while at the right side the gas volume fraction at a vertical cross section plane is shown. It can be seen, as expected, that with increasing pipe elevation the liquid temperature rises and an increasing amount of steam is produced by the wall boiling process. At the upper left corner of Figure 3 (right), it can be seen that the local gas volume fraction ranges between 0.75 and 1.

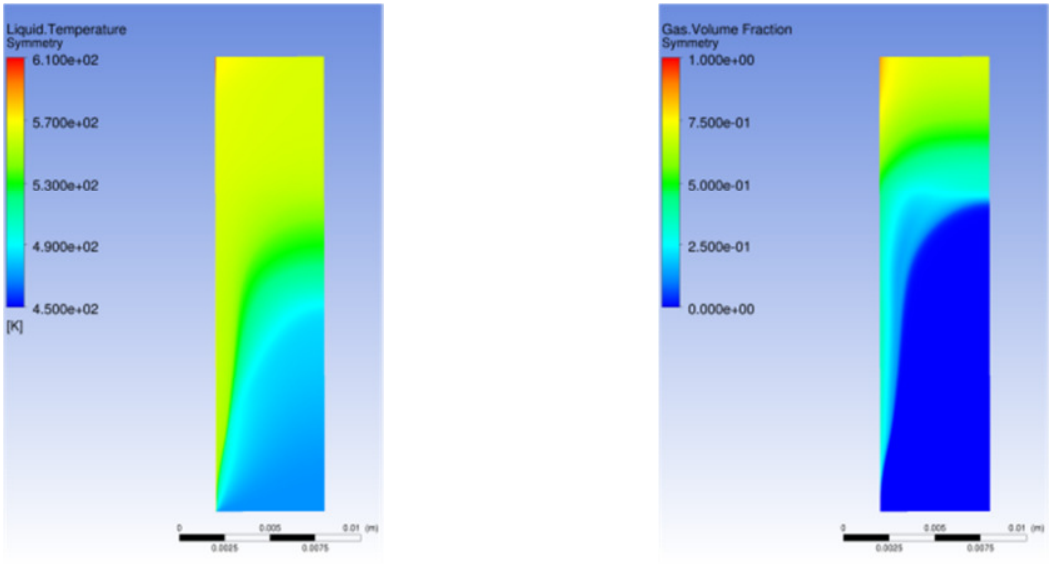

Figure 3 - CFD results obtained with Mesh4. Vertical cross-sectional plane.
Left: Liquid temperature. Right: Gas volume fraction.

On the left side of Figure 4 the influence of the grid resolution can be observed. Cross-sectionally averaged values of the volume fraction are plotted against cross-sectionally averaged values of the thermodynamic quality. Results are compared to the measurements by Bartolomej [3]. The numerical results reproduce very satisfactory the trends of the measurements. Only in the region with larger values of gas volume fraction the quality is slightly over predicted. Profiles obtained with Mesh 3 are already grid independent since they coincide with those of Mesh4, with the only exception of the area where almost no gas is present.
On the right side of Figure 4 the weighting factors (A_{convl}, A_{quench}, A_{evap}, and A_{convg}) are plotted along the heated wall. The blue profile corresponds to A_{convl}, and as expected it is equal to 1 at the inlet (x=0m) where the liquid is still strongly sub-cooled. As the liquid flows upwards it gets warmer and evaporation starts, what leads to an increase of the A_{quench}. For the first ¾ of the pipe the critical gas volume fraction is not reached and A_{convl} keeps decreasing and A_{quench} keeps increasing. However, when

the critical gas volume fraction is reached both values start to decrease while A_{convg} increases very rapidly.

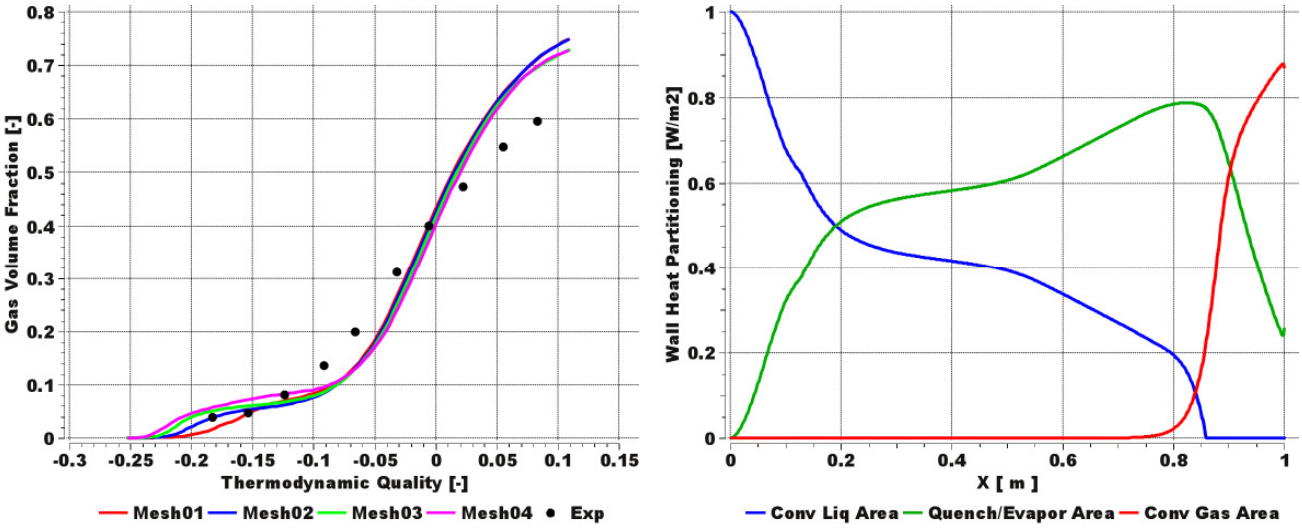

Figure 4 - Left: Grid independence study. Cross averaged values. Gas volume fraction vs. thermodynamic quality. Right: Weight factor distribution along the heated wall.

4.2 The Hoyer Case

4.2.1 Case description

The Hoyer case consists of a vertical pipe with heated wall as well. It has a radius of 5 mm and is 7 m long (Figure 5). The main difference with the Bartolomej case is that the pipe is significantly longer. This causes the fluid in the domain to get much warmer, and even completely evaporate. Hoyer measured wall temperatures. Measurements show very clearly that in the middle of the pipe dry out occurs. The wall temperature stays around saturation for the first 3.5 m and then a dramatic jump in the wall temperature can be observed, indicating that dry out has taken place.

The test conditions for the Hoyer case are summarized in Figure 5. As in the Bartolomej case, the pressure level is at 7 MPa. It must be noted that the inlet temperature or inlet sub-cooling is not specified in the original paper. For this reason, estimation was used. This does not affect the final results. The use of different sub-cooling levels may shift the results upwards or downwards along the pipe. Therefore the results presented in the next section were axially shifted. As a reference point, the onset of the wall temperature jump was used.

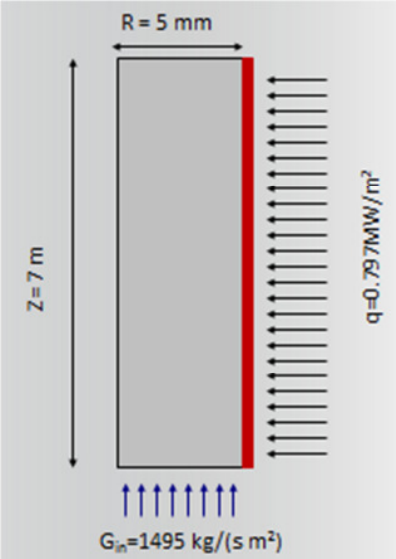

Figure 5 - Sketch of the experimental test facility used by Hoyer [4]

P	G_{in}	q	Subcooling
7.02MPa	1495 kg/(s m^2)	0.797MW/m^2	Unknown

Table 3 - Test conditions of the Hoyer case

4.2.2 CFD-Setup

Two setups were used for the simulations of the Hoyer case. The first CFD setup (setup #1) was essentially the same one as for the Bartolomej case. The only difference was the value of the critical gas volume fraction, which was set to 90% gas volume fraction.

The second setup (setup #2) included two more modifications with respect the first one. The evaluation of the interfacial area density and the liquid and gas heat transfer coefficients was modified. As pointed out in the previous case, the interfacial area density was computed as:

$$6\frac{r_g}{d_p}\ if\ r_g < 0.8; 6\frac{0.8}{d_p}\frac{1-r_g}{1-0.8}\ r_g > 0.8 \quad (13)$$

Where d_P was computed using the correlation by Kurul and Podowski [2].

$$d_P = d_B = \frac{d_1(T_{sub}-T_0)+d_0(T_{sub}-T_1)}{T_1-T_0} \quad (14)$$

However, this correlation was derived for bubbly flow. When the gas content in the domain is very large, we cannot assume that bubbles are present. In such situations gas is not anymore the disperse phase but the continuous one, and inside this continuous phase we can find small droplets. In order to account for this fact, the evaluation of the interfacial area density was change to a blending of formulations. The computation is still based on the expression $6\frac{r_g}{d_p}$, but two different correlations for d_p are used: one for the bubbly regime, i.e. where the gas volume fraction is low and another one for the droplet regime when the gas volume fraction is large. The correlation applied for the droplet regime was derived by Hoyer [4]:

$$d_p = d_D = \frac{2We_c\sigma}{\rho_g U_{sg}^2}\left(\frac{Re}{4{,}6x10^{-7}}\right)^{2/9} \quad (15)$$

And using Eq. (14) and Eq. (15), the new interfacial area density is calculated as:

$$A_{\alpha\beta} = f_B \frac{6r_g}{d_B} + f_D \frac{6r_g}{d_D} \tag{16}$$

Where the factors f_B and f_D are also defined using an exponential function.

$$f_B = \left[1 + e^{50(r_g - r_{g,limit})}\right]^{-1}, f_D = 1 - f_B \tag{17}$$

This strategy was applied for the liquid and gas heat transfer coefficients as well. The liquid heat transfer coefficient was blended between the Ranz-Marshall correlation and a correlation for the droplet regime [4]:

$$htc_l = f_B htc_{l,B} + f_D htc_{l,D} \tag{18}$$

where:

$$htc_{l,B} = \frac{k_l}{d_B}(2 + 0.6Re^{0.5}Pr^{0.33}); \quad htc_{l,D} = \frac{k_l}{d_D}(2 + 0.74Re_D^{0,5}Pr_g^{0,33}) \tag{19}$$

The gas heat transfer coefficient was blended as well using the constant Nusselt number for the bubbly regime and a correlation derived for the droplet regime [4].

$$htc_{gl} = f_B htc_{g,B} + f_D htc_{g,D} \tag{20}$$

where:

$$htc_{g,B} = \frac{k_l}{d_B}26; \; htc_{g,D} = \frac{k_l}{d_D}(0.023Re_{film}^{0.8}Pr_{film}^{1/3}) \tag{21}$$

The improved setup was run with two refined grids, where the main grid parameters are summarized inTable 4.

	Mesh01	**Mesh02**
Cells	20x525	40x1050
Δy^{nw}	2.5x10-^{4}m	1.25x10-^{4}m
Max Y^+ **(setup 2)**	370	190

Table 4 - Parameters of the CFD grids (Hoyer case)

4.2.3 Results and discussion

Figure 6 shows the wall temperature distribution obtained with the first setup and it is compared to the measurements by Hoyer [4]. As mentioned before, due to the lack of information regarding the inlet sub-cooling of the liquid, the CFD results have been shifted in axial direction. The red curve shows the expected behaviour, in the sense that it remains close to saturation temperature until dry out occurs, and then it increases dramatically when dry out takes place. This was due to the use of the extension of the RPI model. However, it can be observed in the measurements, that after the large jump in wall temperature, it decreases about 100K. This last phenomenon was not reproduced in the first simulations. The reason for that was that some of the correlations and models used were derived for bubbly flows. In this case the amount of generated vapour is very large, and near the wall we do not have any more a bubbly flow but a film of vapour covering the wall with some small droplets.

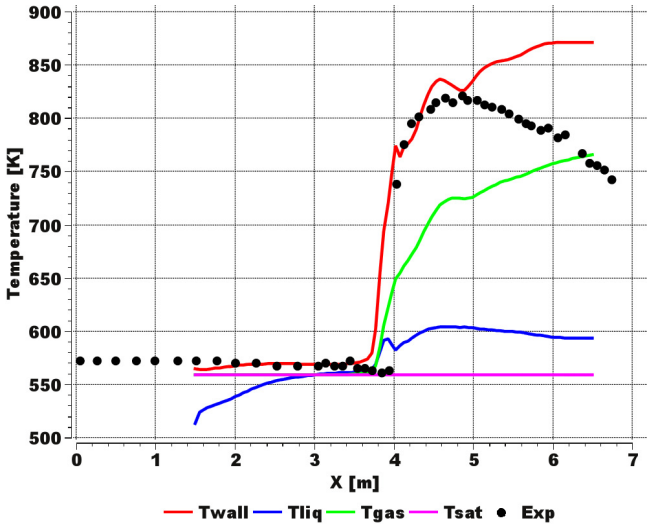

Figure 6 - Hoyer case. Results with setup #1. Wall, liquid, gas, and saturation temperature along the heated wall.

Modifying the setup as indicated in the previous section, better results were obtained. On the left side of Figure 7 the wall temperature distribution obtained with the different meshes is plotted. Both profiles are able to reproduce the increase in the temperature, and now they are also able to predict the decrease of the wall temperature on the upper part of the pipe. On the right side of Figure 7 the wall heat partitioning for the second grid and second setup is shown. As in the Bartolomej case, different regimes can be identified: 1) near the inlet, where convection to liquid is main heat transfer mechanism (blue line is much larger than the others); 2) afterwards there is an area where evaporation and quenching are increasing due to the increase of the wall temperature; and 3) the upper part of the pipe where the main mechanism is now convection to the gaseous phase. In that picture some peaks are visible. The reason is that they lie on the transition zone between the bubbly and droplet regimes. They are numerical artefacts.

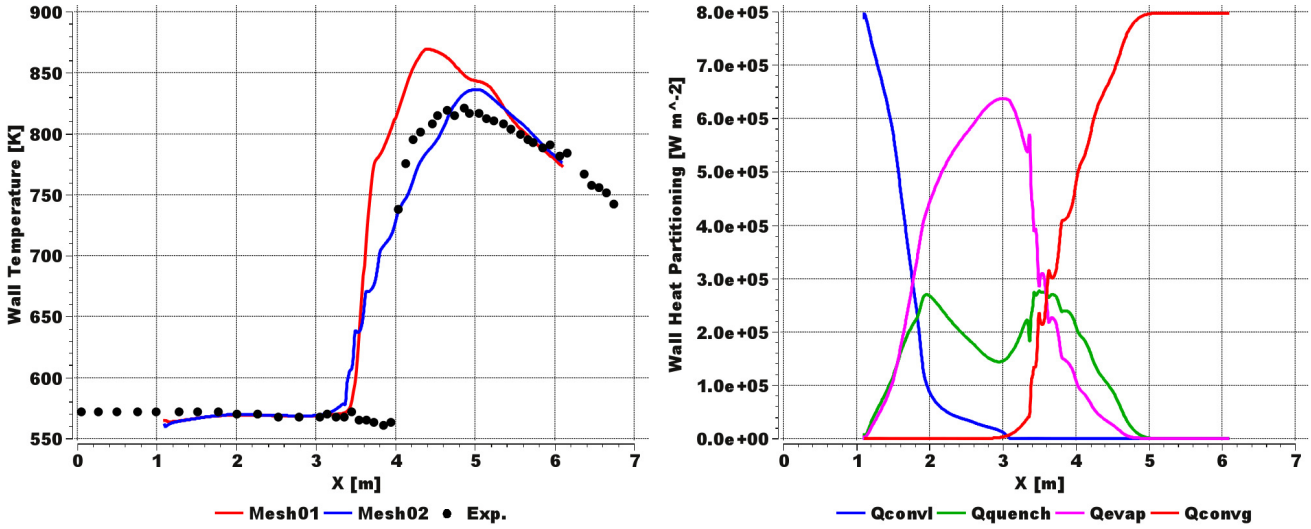

Figure 7: Hoyer case. Results with Setup #2. Left: Wall temperature for the different grids and comparison to measurements. Right: Wall heat partitioning obtained with Mesh2 along the heated wall.

Figure 8 shows contour plots at a vertical cross-sectional plane. On the left side the gas temperature is plotted. It can be seen that in the upper area of the pipe the gas becomes overheated. Gas reaches temperature values of 680 K while saturation temperature is at approx. 570 K. On the right side of Figure 8 the contour plot of the gas volume fraction is included. A steam layer with 100 % vapour is attached to the heated wall shown in the image in red colour.

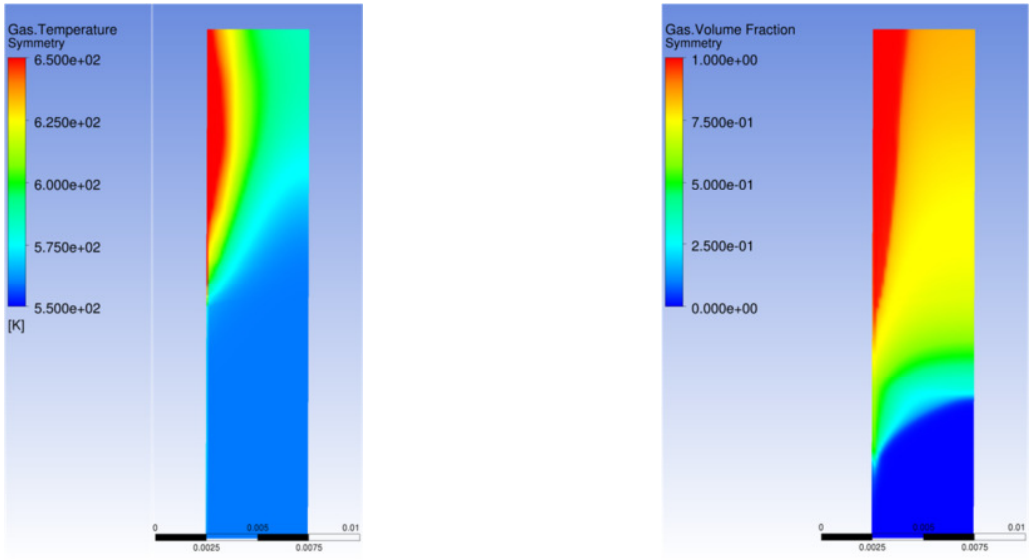

Figure 8: Hoyer case. Results with setup #2. Vertical cross-sectional plane.
Left: Gas temperature. Right: Gas volume fraction.

5. CONCLUSIONS

An extension of the RPI wall boiling model has been derived and implemented. This modification is aimed to be used in a wider range of applications, including those where the content of vapour near the wall is large or even so large that the wall is completely covered by a layer of vapour.

The new formulation of the RPI model includes a fourth heat flux mechanism to extract heat from the heated wall, i.e. convection to the vapour phase. Therefore a fourth wall heat flux component is included in the wall heat partitioning.

To validate the model two cases from the literature were chosen. The Bartolomej case allowed us to check the prediction of gas volume fraction and the Hoyer case the wall temperature prediction. Agreement between CFD results and Bartolomej measurements was satisfactory. In the case by Hoyer it was required to modify the evaluation of some parameters in addition to the use of the extended RPI model. The modified variables were the interfacial area density, the liquid heat transfer coefficient and the gas heat transfer coefficient, which have a large impact on the prediction of the interphase transfer phenomena. With these adaptions, CFD results were very close to the measurements and were always in less than 10 K difference to them.

6. REFERENCES

[1] N. Kurul, M. Podowski. “On the modeling of multidimensional effects in boiling channels”, 27th National Heat Transfer Conference. Minneapolis.1991.

[2] ANSYS Inc.”ANSYS CFX 14.0. Theory users manual”. Canonsburg, USA.

[3] G. Bartolomej. “An experimental investigation of true volumetric vapour content with subcooled boiling in tubes”, Thermal Engineering, vol. 29, num. 2, pp. 132-135,1982.

[4] N. Hoyer. “Calculation of dry out and post-dry out heat transfer for tube geometry”, International Journal of Multiphase Flow. vol. 24, num. 2, pp. 319-334,1982.

[5] NEA/CSNI. “Best Practice Guidelines for the use of CFD in Nuclear Reactor Safety Applications”, NEA/CSNI/R(2007)5.

[6] C. Lifante, F. Reiterer, Th. Frank, „Coupling of Wall Boiling with Discrete Population Balance Model”. Journal of Computational Multiphase Flows. Vol. 4. Num. 3. 2012.

[7] H. Li, S. Vasquez, H. Punekar, R. Muralikrishnan. “Prediction of boiling and critical heat flux using an eulerian multiphase boiling model”. Proceedings of the ASME 2011 International Mechanical Engineering Congress & Exposition 2011. November 11-17, 2011, Denver, Colorado, USA.